

# Maximum power point tracking based on improved spotted hyena optimizer for solar photovoltaic

Muhammad Farizky Alvianandy, Novie Ayub Windarko, Bambang Sumantri

Department of Electrical Engineering, Politeknik Elektronika Negeri Surabaya, Surabaya, Indonesia

## Article Info

### Article history:

Received Aug 31, 2021

Revised Jul 23, 2022

Accepted Aug 9, 2022

### Keywords:

Maximum power point tracker

Partial shading condition

Photovoltaic

Powersim

Spotted hyena optimizer

## ABSTRACT

The conventional maximum power point tracking (MPPT) method such as perturb and observe (P&O) under partial shading conditions with non-uniform irradiation, can get trapped on local maximum power point (LMPP) and cannot reach global maximum power point (GMPP). This study proposes a bio-inspired metaheuristic algorithm spotted hyena optimizer (SHO) and improved SHO as a new MPPT technique. The proposed SHO-MPPT and improved SHO-MPPT are used to extract GMPP from solar photovoltaic (PV) arrays operated under uniform irradiation and non-uniform irradiation. Simulation with Powersim (PSIM) and experimental with the emulated PV source were presented. Furthermore, to evaluate the performance of the proposed algorithm, SHO-MPPT is compared with P&O-MPPT and particle swarm optimization (PSO)-MPPT. The SHO-MPPT has an accuracy of 99% and has the good capability, but there are power fluctuations before reaching MPP. Therefore, improved SHO-MPPT was developed to get better results. The improved SHO-MPPT proved high accuracy of 99% and faster than SHO-MPPT and PSO-MPPT in tracking the maximum power point (MPP). Furthermore, there are minor power fluctuations.

This is an open access article under the [CC BY-SA](https://creativecommons.org/licenses/by-sa/4.0/) license.



## Corresponding Author:

Muhammad Farizky Alvianandy

Department of Electrical Engineering, Politeknik Elektronika Negeri Surabaya

Raya ITS-Kampus PENS Street, Surabaya, 60111, Indonesia

Email: pondokmulia@gmail.com

## 1. INTRODUCTION

Renewable energy sources are an important role as a solution for dependence on fossil fuel. Therefore, a worldwide special attention was devoted to clean energy especially through energy efficiency plans, involving low carbon products and services [1]. Many countries are already using renewable energy sources for electricity generation because they consider the impacts of climate change that fossil fuels can cause. The growth of renewable energy technology is driven by the increasing price of fossil fuels and CO<sub>2</sub> emissions produced [2]. Photovoltaic (PV) systems are one of the most popular renewable energy sources. PV converts solar power into electricity. There are many types of technologies used to generate electricity based on the PV principle. Crystalline silicon is the main technology used commercially, but there are other technologies that are under intense research to produce more efficient solar cells [3].

PV systems have advantages converting solar energy to electricity which is abundant, inexhaustible and clean. PV systems also have disadvantage of not having the reliability of capturing solar energy. PV array is an interconnected system of PV modules. The output power of the PV array is affected by environmental conditions including solar irradiation and temperature. In a wide area, there are several conditions where the PV module is covered by clouds and leaves. this condition causes partial shading and non-uniform irradiation. The output power characteristic of PV under partial shading condition exhibits

multiple peaks: a single global maximum power point (GMPP) and several local maximum power point (LMPP) [4].

To enhance the efficiency of the PV systems and get maximum power from solar PV the maximum power point tracking (MPPT) technique is needed. Several conventional MPPT techniques include constant voltage tracking (CVT) [5], open-circuit voltage tracking (OVT) [6], perturb and observe (P&O) [7]–[9], and incremental conductance (IC) [10]. may fail to track GMPP and trapped at LMPP. Many advanced methods based on artificial intelligence have been proposed, such as fuzzy logic control, artificial neural network (ANN), genetic algorithm (GA) [11], differential evolution (DE) [12], gray wolf optimizer (GWO) [13], salp swarm algorithm (SSA) [14], ant colony optimization (ACO) [15], artificial bee colony (ABC) [16], particle swarm optimization (PSO) [17] can successfully applied to track GMPP. In addition new metaheuristic algorithms such as manta ray foraging optimization (MRFO) [18], a bat algorithm (BA) [19] have been developed and applied for MPPT.

The spotted hyena optimizer (SHO) is a metaheuristic optimization algorithm inspired by the behavior of spotted hyenas. The main concept behind this algorithm is the social relationship between spotted hyenas and their collaborative behavior. The three basic steps of the SHO are searching for prey, encircling and attacking prey. These three are mathematically modeled and implemented. SHO algorithm has better statistical results than GWO, PSO, moth-flame optimization (MFO), multi-verse optimizer (MVO), sine cosine algorithm (SCA), gravitational search algorithm (GSA), genetic algorithm (GA), and harmony search (HS) methods in solving optimization problems. SHO algorithm also requires less computation to find optimal solutions [20]. Therefore, the SHO algorithm and improved SHO algorithm are proposed for MPPT to enhance the performance and efficiency of PV system.

## 2. PV AND BUCK CONVERTER MODELLING

### 2.1. PV cell modelling

One popular model of PV cells is a single diode equivalent circuit model. The equivalent circuit of this model consists of a parallel current source, a diode parallel to the current source, and two resistors namely a parallel resistor ( $R_{sh}$ ) and a series resistor ( $R_s$ ), as shown in Figure 1. These two resistors reflect the value of the internal resistance of the cell. This PV cell model represents the electrical behavior of p-n junction [21].

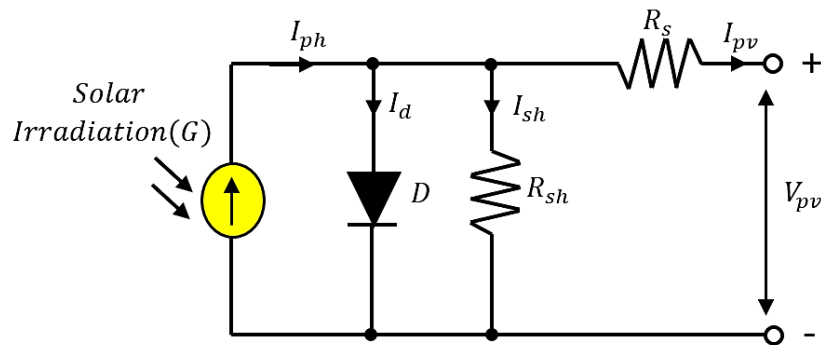


Figure 1. Single diode model for equivalent circuit of the PV

From the single diode equivalent circuit, the output current of PV module can be expressed:

$$I_{pv} = I_{ph} - I_D - I_{sh} \quad (1)$$

$$I_D = I_s \left( e^{q \frac{V_D}{\eta k T_0}} - 1 \right) \quad (2)$$

$$R_{sh} = \frac{V_D}{I_{sh}} \quad (3)$$

$$V_D = V_{pv} + I_{pv} \cdot R_s \quad (4)$$

$$I_{ph} = \frac{G}{1000}(I_{sc} + C_T(T - T_0)) \tag{5}$$

$I_{pv}$  is resulted by  $I_{ph}$ ,  $I_D$  and  $I_{sh}$  represented in (1).  $I_{pv}$  and  $V_{pv}$  are the current and voltage of PV cell modul,  $I_{ph}$  is direct current (DC) source model for electrical current produced by solar irradiation,  $I_D$  is internal diode current and  $I_{sh}$  is shunt resistance current.  $I_D$  is represented in (2).  $I_s$  is the dark saturation current of the PV cell,  $V_D$  is internal diode voltage,  $q$  is the electrical charge constant ( $1.6 \times 10^{-9}C$ ),  $\eta$  is the diode quality factor,  $k$  is Boltzman's constant ( $1.38 \times 10^{-23} J/K$ ) and  $T_0$  is temperature in standard test condition.  $I_{sh}$  is represented in (3).  $V_D$  is represented in (4).  $R_s$  and  $R_{sh}$  are series and shunt resistors of PV cell.  $R_s$  and  $R_{sh}$  represent an internal resistance and leakage resistance.  $I_{ph}$  is represented in (5).  $I_{sc}$  is the short circuit current value in the solar panel,  $G$  is the solar irradiation value ( $W/m^2$ ),  $T$  is the ambient temperature, and  $C_T$  is temperature coefficient.

**2.2. PV module characteristic**

The PV module characteristics are modeled with I-V characteristics and P-V characteristics. The maximum power that PV module can produce depends on environmental conditions of solar irradiation and temperature. The specifications of PV module in Table 1 provide in standard test conditions (STC) where solar irradiation  $1,000 W/m^2$  and cell temperature  $25^\circ C$ . The PV module used has a capacity of 100 W with a maximum voltage of 17.6 V volts and a maximum current of 5.62 A. The P-V curve with the difference solar irradiation values is shown in Figure 2. PV module will reach their maximum power when the solar irradiation value is  $1,000 W/m^2$  and cell temperature  $25^\circ C$ . The I-V curve of PV module at STC condition is shown in Figure 3.

Table 1. PV module specifications

No	Parameter	Symbol	Value
1.	Maximum power	$P_{max}$	100 W
2.	Maximum power voltage	$V_{mp}$	17.6 V
3.	Maximum power current	$I_{mp}$	5.69 A
4.	Open circuit voltage	$V_{oc}$	22.6 V
5.	Short circuit current	$I_{sc}$	6.09 A
6.	Ambient temperature	T	$25^\circ C$
7.	Solar irradiation	G	$1,000 W/m^2$

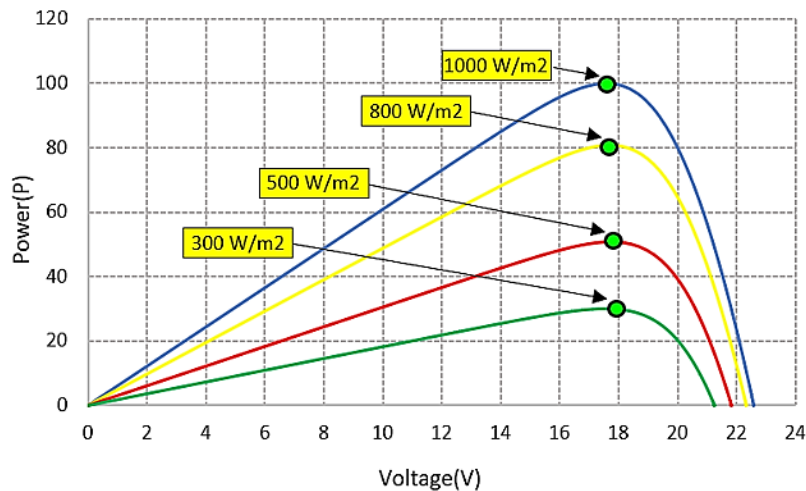


Figure 2. P-V characteristic of PV module

**2.3. Partial shading condition**

Partial shading occurs when the PV array receives non-uniform irradiation. Such a situation occurs due to the shadow of clouds, trees, tall buildings, and other objects that fall on the particular portions of the PV [22]–[24]. The power generated from panels with partial shading is lower than panels without partial shading. Multiple peaks occur in the power-voltage (P-V) curve during partial shading conditions. Figure 4 shows the PV characteristics in uniform and non-uniform irradiation conditions, where black dots show the

GMPP and black triangles show the LMPP. PV array consists of five PV modules with the number of maximum MPP is five. Under uniform irradiation, the PV array generate a single MPP. Contrary to partial shading, the PV array generates LMPP and GMPP.

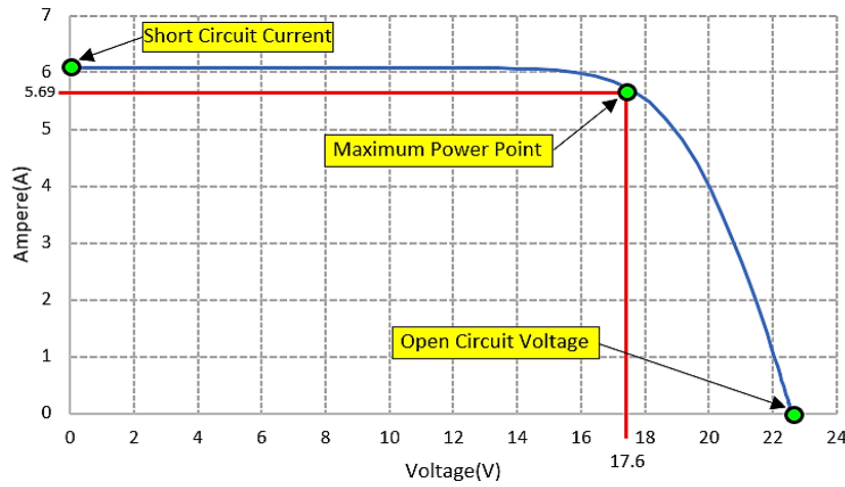


Figure 3. I-V characteristic of PV module

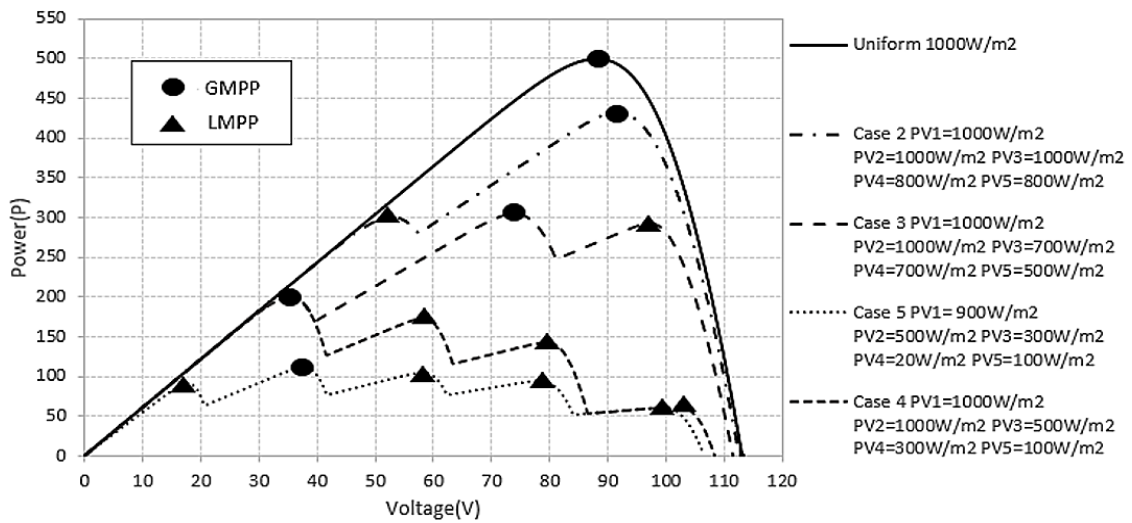


Figure 4. P-V characteristics under uniform and non-uniform irradiation

### 3. BUCK CONVERTER

The electrical circuit of the buck converter is shown in Figure 5. DC-DC buck converter is one of the converters to control the DC output voltage. Buck-converter is a step-down converter or DC voltage reducer that implements a switching mode power supply (SMPS) system. It is a converter with higher efficiency when compared to ordinary voltage-reducing power supply (linear system).

The buck converter circuit can be formulated by (6)–(10) [25]:

$$V_o = D \cdot V_i \tag{6}$$

$$D = \frac{t_{on}}{T_s} \tag{7}$$

$$L_{min} = \frac{(1 - D)R}{2f} \tag{8}$$

$$L_f = \left( \frac{V_i - V_o}{\Delta I_L f} \right) D \quad (9)$$

$$C_f = \frac{1-D}{8L \left( \frac{\Delta V_o}{V_o} \right) f^2} \quad (10)$$

where  $V_o$  and  $V_i$  are the output and input voltages,  $D$  is the duty cycle.  $V_o$  represented in (6). The buck converter produces an output voltage that is less than or equal to the input voltage.  $t_{on}$  is PWM signal duration to turn on buck converter switch.  $T_s$  is switching periode.  $D$  represented in (7).  $L_{min}$  is the minimum inductance needed for continuous current operation,  $R$  is load resistance and  $f$  is the switching frequency.  $L_{min}$  represented in (8).  $L_f$  and  $C_f$  are the inductor and capacitor filter, respectively.  $\Delta I_L$  is the inductor ripple current.  $L_f$  represented in (9).  $\Delta V_o$  is the load voltage ripple.  $C_f$  represented in (10). When duty cycle 0% means open circuit and when duty cycle 100% means short circuit. The specifications of the DC-DC buck converter used are shown in Table 2.

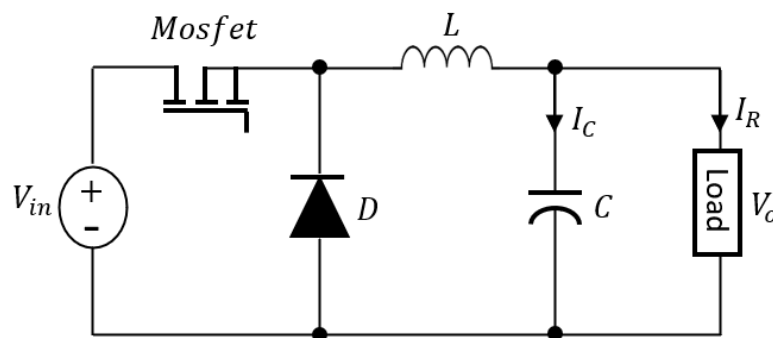


Figure 5. Buck converter electrical circuit

Table 2. The specifications of buck converter

No	Parameter	Symbol	Value
1	Switching frequency	f	20 kHz
2	Resistor	R	3.526 $\Omega$
3	Inductor	L	1.1 mH
4	Capacitor	C	177.15 $\mu$ F

#### 4. PROPOSED METHOD SPOTTED HYENA OPTIMIZATION (SHO)

In this research, the SHO algorithm and improved SHO were proposed for the MPPT. The application of the SHO algorithm for MPPT is expected solve the problem of the conventional MPPT method can being stuck at the local maximum power point (LMPP). The experiments test was used emulated PV source, emulated PV source is one of the PV testing techniques with unilluminated solar PV and can be carried out in the laboratory using a DC power supply. The block diagram for this research is displayed in Figure 6.

The spotted hyena optimizer is a novel proposed metaheuristic swarm intelligence optimization method for solve optimization problems. Spotted Hyenas are large dog-like carnivores. They live in savannas, grasslands, sub-deserts and forests of both Africa and Asia. They have an ability to fight endlessly over territory and food. The main steps of SHO are inspired by hunting behavior of spotted hyenas [21].

##### 4.1. Mathematical model and optimization algorithm

Spotted hyenas are social animals that can communicate with each other through specialized calls such as postures and signals. The spotted hyena track prey by sight, hearing, and smell. In this sub-section, the mathematical model of the hunting mechanism of the spotted hyenas is divided into four steps, namely encircling prey, hunting, attacking prey (exploitation) and search prey (exploration).

##### 4.1.1. Encircling prey

Spotted hyena can be familiar with the location of prey and encircle them. The spotted hyena which near to the prey is the current best candidate and initially is optimum solutions, and according to it the other

spotted hyena will update their positions. The mathematical modeling for this phenomenon is represented as (11), (12):

$$\vec{D}_h = |\vec{B} \cdot \vec{P}_p(t) - \vec{P}(t)| \quad (11)$$

$$\vec{P}(t+1) = \vec{P}_p(x) - \vec{E} \cdot \vec{D}_h \quad (12)$$

where,  $\vec{D}_h$  is the distance of the spotted hyena and the prey,  $\vec{B}$  and  $\vec{E}$  are the coefficient vectors,  $\vec{P}_p$  indicates the position vector of prey,  $t$  is the current iteration, and  $\vec{P}$  is the position vector of spotted hyena. The coefficient vector can be calculated as (13), (14):

$$\vec{E} = 2\vec{h} \cdot r\vec{d}_1 - \vec{h} \quad (13)$$

$$\vec{B} = 2 \cdot r\vec{d}_2 \quad (14)$$

$$\vec{h} = 5 - \left( \text{Iteration} * \left( \frac{5}{\text{MaxIteration}} \right) \right) \quad (15)$$

where,  $\vec{h}$  is linearly decrease from 5 to 0 as increase the iteration, the decrease  $\vec{h}$  is for balancing the exploration and exploitation.  $r\vec{d}_1$  and  $r\vec{d}_2$  are the random vectors in range [0, 1].

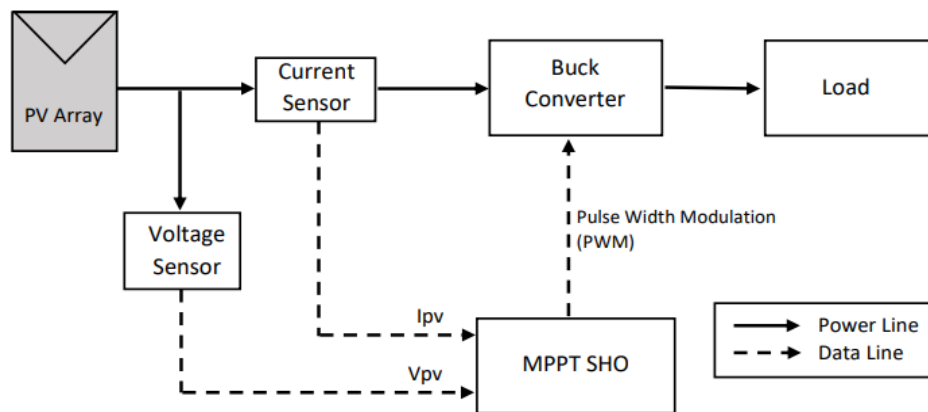


Figure 6. Block diagram of PV system

#### 4.1.2. Hunting

Spotted hyenas usually live and hunt in groups and can identify the location of prey. To get a mathematical model of hunting behavior, the best search agent is the optimal solution and knows the location of prey. The other search agents create clusters towards the best search agents and saved the best solutions obtained so far. The mathematical modeling for hunting is represented as (16)-(18):

$$\vec{D}_h = |\vec{B} \cdot \vec{P}_h - \vec{P}_k| \quad (16)$$

$$\vec{P}_k = \vec{P}_h - \vec{E} \cdot \vec{D}_h \quad (17)$$

$$\vec{C}_h = \vec{P}_k + \vec{P}_{k+1} + \dots + \vec{P}_{k+N} \quad (18)$$

where,  $\vec{P}_h$  and  $\vec{P}_k$  defines the position of first best spotted hyena and other spotted hyena.  $N$  is the total number of spotted hyena which is represented as (19):

$$N = \text{count}_{noh}(\vec{P}_h, \vec{P}_{h+1}, \vec{P}_{h+2}, \dots, (\vec{P}_k + \vec{M})) \quad (19)$$

where,  $\vec{M}$  is a random vector in range of [0.5, 1],  $noh$  is the number of solution,  $count_{noh}$  is count all candidate solution after addition with  $\vec{M}$ , and  $\vec{C}_h$  is a cluster of  $N$  number of optimal solution.

#### 4.1.3. Attacking prey

The mathematical formulation for attacking the prey is represented as (20):

$$\vec{P}(t+1) = \frac{\vec{C}_h}{N} \quad (20)$$

where  $\vec{P}(t+1)$  save the best solution and updates the position of other search agents according to the position of the best agent. The spotted hyena attacks the prey constantly update their position.

#### 4.1.4. Search prey

Spotted hyenas usually search prey according to the position of cluster spotted hyena, which is vector  $\vec{C}_h$ . Vector  $\vec{E}$  half of iteration is use for searching (exploration) and the other half is use for hunting (exploitation). When  $|\vec{E}| \geq 1$  is for exploration and when  $|\vec{E}| \leq 1$  is for exploitation to get best solution.

### 4.2. The proposed improved SHO

The purpose of improved SHO algorithm in this study is to improve performance in tracking MPP by reducing the time to track MPP, high efficiency and more stable. Based on the SHO algorithm's mathematical model, vector  $\vec{B}$  is has a random value that will affect the SHO to avoid stuck in local optima not only at the beginning of the iteration but also at the end of the iteration. Vector  $\vec{B}$  can cause the SHO search agent to approach the optimal solution at the end of the iteration, it can cause more time needed for all search agents to settle at GMPP. Therefore, to improve SHO performance in tracking MPP and reducing the time needed for all search agents to settle at GMPP, in the improved SHO-MPPT vector  $\vec{B}$  which is in the (11) and (16) is removed and changed to (21) and (22).

$$\vec{D}_h = |\vec{P}_p(t) - \vec{P}(t)| \quad (21)$$

$$\vec{D}_h = |\vec{P}_h - \vec{P}_k| \quad (22)$$

In addition, other factors that can affect the stability and time to reach MPP are vector  $\vec{E}$ , where vector  $\vec{E}$  allows the spotted hyena agent to move away from prey or optimal solution, it can cause spotted hyena search agent need more time to approach the optimal solution. The value of the vector  $\vec{E}$  is affected by vector  $\vec{h}$ . Vector  $\vec{h}$  value is linearly decrease from 5 to 0 as increase the iteration. Therefore, to get faster results in tracking MPP, it can be by setting the range of vector  $\vec{h}$ , if the value vector  $\vec{h}$  is small then the value of vector  $\vec{E}$  is also small and the spotted hyena search agent can approach the optimal solution faster. In this study vector  $\vec{h}$  value is tested from the range [5, 0], [4, 0], [3, 0], [2, 0] and [1, 0]. The purpose of the test is to get the best range vector  $\vec{h}$  value for MPPT.

### 4.3. Steps and flowchart of improved SHO

The flowchart of improved SHO-MPPT is shown in Figure 7, and the steps of improved SHO algorithm are summarized as:

- Step 1: initialize the spotted hyenas population  $Pi(i = 1, 2, \dots, n)$ .
- Step 2: initialize SHO parameters and the maximum number of iterations.
- Step 3: calculate the fitness value of each search agent
- Step 4: define the group of optimal solutions using (18) and (19).
- Step 5: update the positions of search agents using (17), (20) and (21).
- Step 6: if there is a search agent that passes from the boundary, then adjust it.
- Step 7: calculate the fitness value of each search agent
- Step 8: update the position of search agent if there is a better solution then previous optimal solution.
- Step 9: update the group of spotted hyenas  $Ch$ .
- Step 10: if the stopping criterion is met, the algorithm will be stopped. Otherwise, the operation is repeated from Step 4. This process is continued until the stopping criterion is satisfied.
- Step 11: return the best optimal solution, after stopping criteria is satisfied.

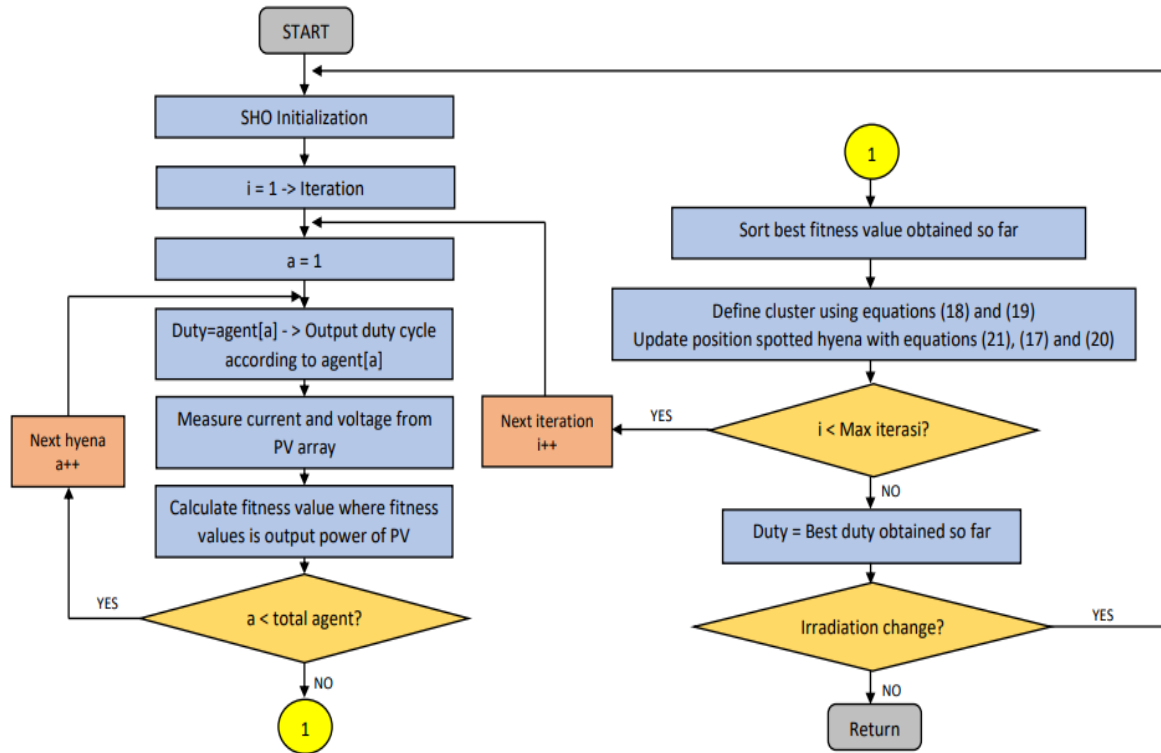


Figure 7. Flowchart of improved SHO-MPPT

## 5. SIMULATIONS AND EXPERIMENTAL RESULTS

The proposed algorithm is simulated using Powersim (PSIM), a simulation solution for all power electronics applications. Figure 8 shows MPPT simulation circuit consists of 5 PV modules in PSIM. The specifications of the DC-DC buck converter used are shown in Table 2. The PV string consist of 5 PV modules are used to simulate non-shading and partial shading condition. Several MPPT algorithms are designed and tested, including P&O, PSO, SHO, and improved SHO. The test was carried out for several conditions. The test conditions are as:

- Case 1 is a uniform irradiation test, PV array is operated at STC where the solar irradiation and temperature value is set constant at 1,000 W/m<sup>2</sup> and 25 °C. The maximum power that can be generated is 500.28 W.
- Case 2 is partial shading condition with non-uniform irradiation test, the temperature is set constant at 25 °C and the solar irradiation value is set PV1=900 W/m<sup>2</sup>, PV2=500 W/m<sup>2</sup>, PV3=300 W/m<sup>2</sup>, PV4=200 W/m<sup>2</sup> and PV5=100 W/m<sup>2</sup>. The maximum power that can be generated is 110.69 W.

To get the best vector  $\vec{h}$  value for improved SHO-MPPT, vector  $\vec{h}$  value is tested from the range [5, 0], [4, 0], [3, 0], [2, 0] and [1, 0]. The best value from this test will be used for test in cases 1-2. The condition for this test is uniform irradiation. PV array is operated at STC where the solar irradiation and temperature value is set constant at 1,000 W/m<sup>2</sup> and 25 °C. The maximum power that can be generated is 500.28 W. Figure 9 shows the results of PV output power and duty cycle for vector  $\vec{h}$  value test.

To test the performance of the algorithm, several comparison methods are tested. Algorithm performance is analyzed based on the accuracy value in tracking MPP, time to reach the MPP, efficiency and stability. The following method parameters used in the simulation are shown in Table 3.

As shown in Figure 9 vector  $\vec{h}$  with value range [1, 0] can track MPP at  $t=0.64$  s. There is also less fluctuation power. In MPP condition there is no oscillation. The maximum power is 489.1 W with and accuracy value of 97.76%. Vector  $\vec{h}$  with value range [2, 0] can track MPP at  $t=0.58$  s. There is also less fluctuation power. In MPP condition there is no oscillation. The maximum power is 500,25W with and accuracy value of 99.99%. Vector  $\vec{h}$  with value range [3, 0] can track MPP at  $t=0.95$  s. In MPP condition there is no oscillation. Before reach the MPP, there is fluctuation power. The maximum power is 500,12 W with and accuracy value of 99.99%. Vector  $\vec{h}$  with value range [4, 0] can track MPP at  $t=1.17$  s. In MPP condition there is no oscillation. Before reach the MPP, there is fluctuation power. The maximum power is

499.6 W with an accuracy value of 99.86%. Vector  $\vec{h}$  with value range [5, 0] can track MPP at  $t=1.11$  s. In MPP condition there is no oscillation. Before reaching the MPP, there is fluctuation in power. The maximum power is 500.17 W with an accuracy value of 99.97%. Based on the test results, the vector  $\vec{h}$  value which shows the best performance for MPPT is vector  $\vec{h}$  with value range [2, 0]. The vector  $\vec{h}$  value with range [2, 0] will be used to test in cases 1–3.

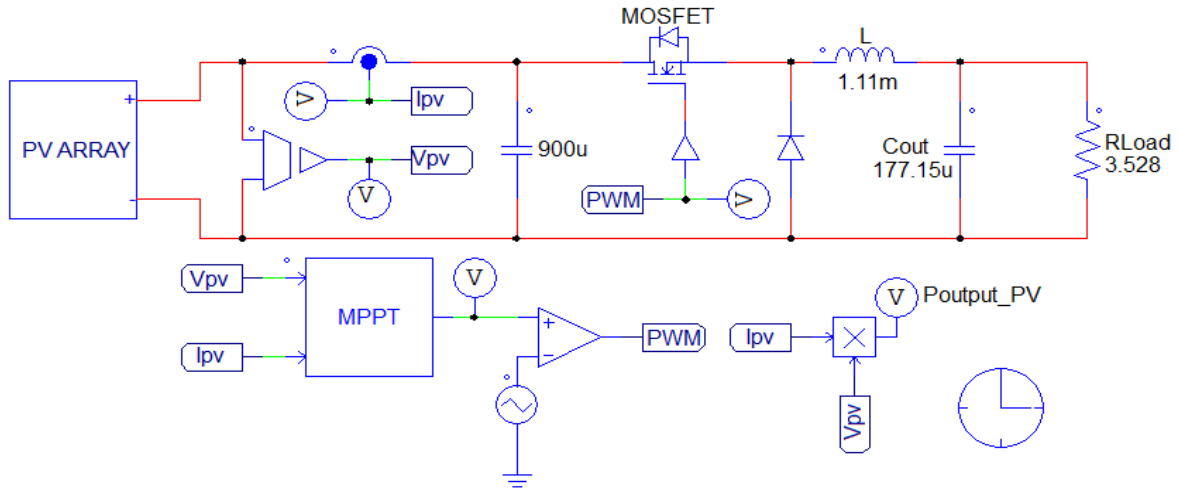


Figure 8. MPPT simulation circuit consists of 5 PV modules in PSIM

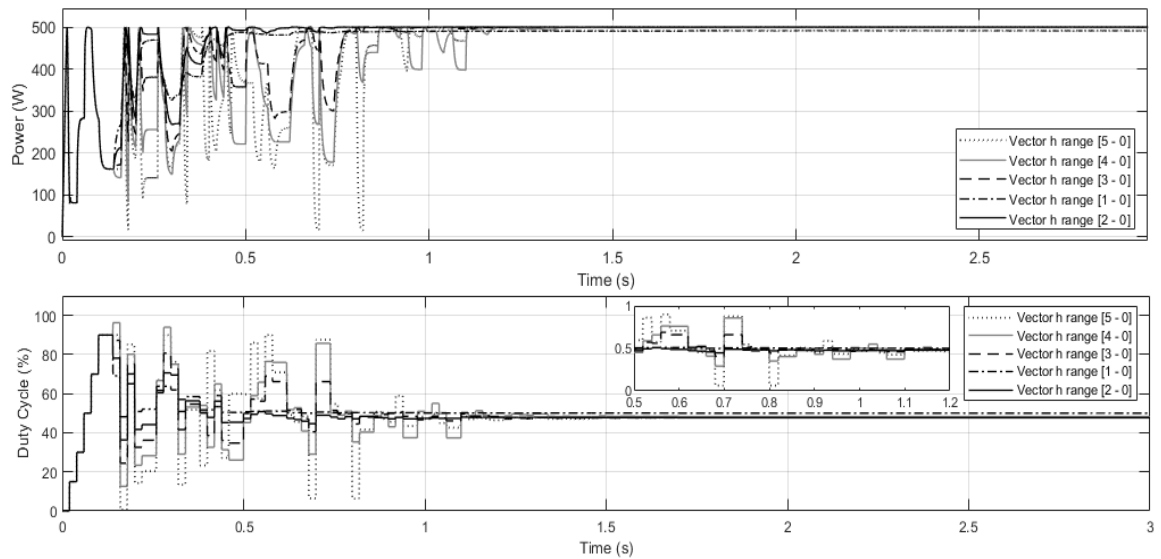


Figure 9. vector  $\vec{h}$  value for improved SHO-MPPT

Table 3. Method parameters used

Method	Parameter	Value
P&O	Duty cycle start	0%
	Duty cycle step	3%
PSO	Number of search agent	5
	Duty cycle initialization	{0.05, 0.2, 0.5, 0.7, 0.9}
	Max iteration	15
SHO	C1, C2, W	1.2, 1.4, 0.5
	Number of search agent	5
Improved SHO	Duty cycle initialization	{0.15, 0.3, 0.5, 0.7, 0.9}
	Max iteration	15

As shown in Figure 10 the results of case 1, P&O, PSO, SHO and improved SHO can track the MPP where the maximum power value of case 1 is 500.2 W. What makes different is time to track MPP and power fluctuations. The P&O can reach MPP rapidly at  $t=0.35$  s, but there are oscillations at MPP conditions where it can increase power losses. The power oscillation value in MPP conditions ranges 499.86–462.3 W. PSO can track MPP at  $t=1.26$  s, and there is no oscillation during the MPP condition. In the MPP condition, the output power is 499.6 W with an accuracy value of 99.86%. SHO can track MPP correctly at  $t=1.71$  s, and there is no oscillation during the MPP condition, but before reaching MPP, there are fluctuation power. In the MPP condition, the output power is 497.6 W with an accuracy value of 99.48%. Improved SHO can track MPP at  $t=0.45$  s and faster than PSO and SHO. There is no oscillation during the MPP condition. Before reaching MPP, there is also less fluctuation power. In the MPP condition, the output power is 500.26 W with an accuracy value of 99.99%.

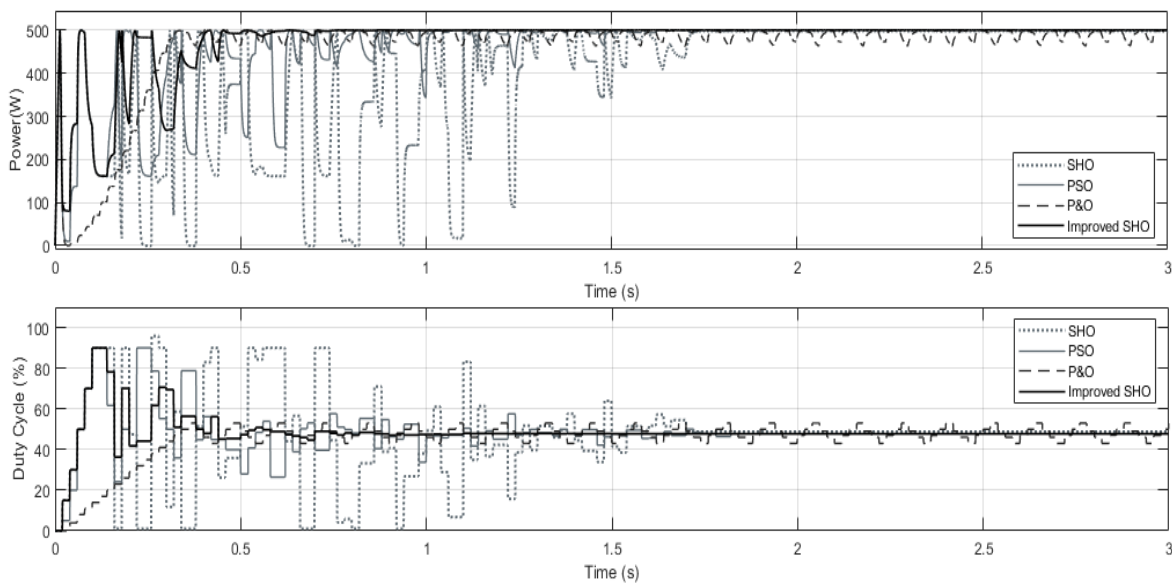


Figure 10. Case 1 uniform irradiation test at STC

As shown in Figure 11 the results of case 2, P&O fail to reach the GMPP and stuck in LMPP, and the other algorithm can reach the GMPP at different time. The maximum power of P&O is 91.3 W, and there is oscillation at MPP condition, where it can increase power losses. PSO can track MPP correctly at  $t=1.73$  s, and there is no oscillation during the MPP condition, but before reaching MPP, there are fluctuation power. In the MPP condition, the output power is 110.65 W with an accuracy value of 99.96%. SHO can track MPP correctly at  $t=1.72$  s, and there is no oscillation during the MPP condition, but before reaching MPP, there are fluctuation power and duty cycles. In the MPP condition, the output power is 109.8 W with an accuracy value of 99.2%. Improved SHO can track MPP at  $t=0.77$  s and faster than PSO and SHO. There is no oscillation during the MPP condition. Before reaching MPP, there is also less fluctuation power. In the MPP condition, the output power is 110.4 W with an accuracy value of 99.74%.

From the results of simulation for cases 1 and 2, the comparison data of four methods is obtained as shown in the Table 4. To evaluate and verify the performance of the proposed Improved SHO-MPPT and SHO-MPPT, experiments are conducted in a laboratory setup with unilluminated solar PV technique. The experimental prototype was built as shown in Figure 12. Experimental circuit consists of 3 PV connected in series. The microcontroller STM32F746G Discovery was used to provide PWM signal for dc-dc converter. The load was used Rigol DL3021 dc electronic load. The sensor was used is ACS712-20A and voltage divider for current and voltage sensor. The result of maximum power was measured with digital multimeter and clamp meter.

The experiments tests were performed on experimental prototypes, the proposed improved SHO-MPPT and SHO-MPPT was presented. The method parameter used for the test is in Table 3. Figure 13 shows the PV output performance under partial shading with non-uniform irradiation  $1,000 \text{ W/m}^2$ ,  $600 \text{ W/m}^2$  and  $400 \text{ W/m}^2$ . The maximum power for this case is 133.4 W. Therefore, the sampling time value between the simulation and the experiment is different, this is needed to obtain accurate PV output current. The sampling

time was used for the simulation is 0.02 s and for the experiment is 0.5 s. Figure 13(a) shows the performance improved SHO-MPPT and Figure 13(b) shows the performance SHO-MPPT test under partial shading condition. The proposed improved SHO-MPPT can track MPP faster and reduce fluctuation power compare to SHO-MPPT. Time of tracking MPP improved SHO-MPPT is 31 s and SHO-MPPT is 46 s. The maximum power improved SHO-MPPT is 132.61 W and SHO-MPPT is 132.26 W, from that result the accuracy of improved SHO-MPPT and SHO-MPPT for tracking the MPP is above 99%.

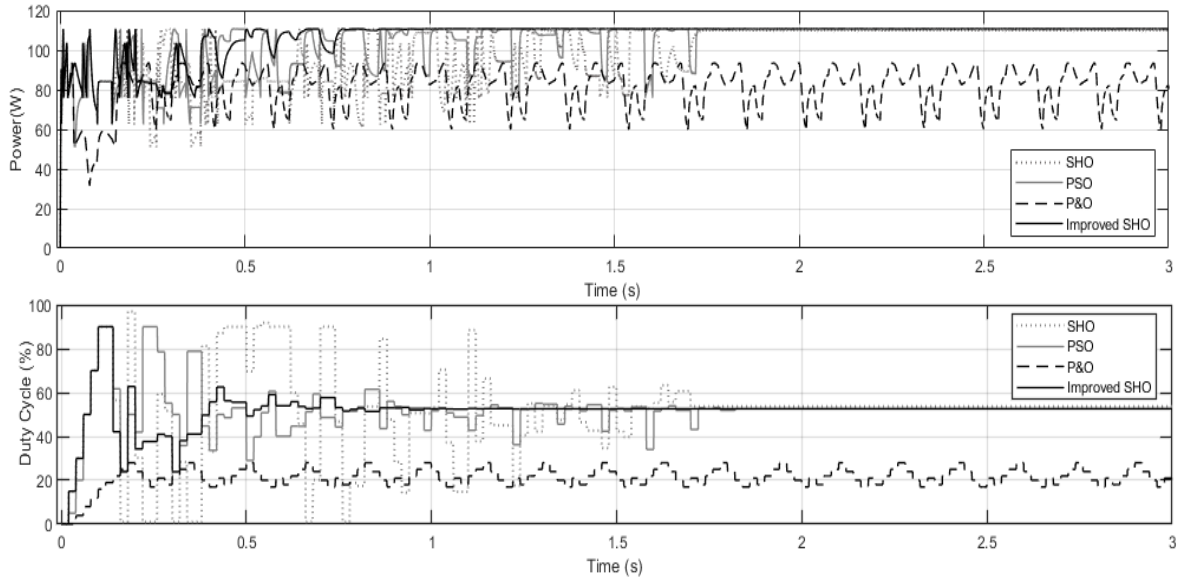


Figure 11. Case 2 partial shading with non-uniform irradiation test

Table 4. Comparison of test results

Case	GMPP		P&O		PSO		SHO		Improved SHO				
	$P_{max}$ (W)	$P_{mppt}$ (W)	Accuracy (%)	Time (s)	$P_{mppt}$ (W)	Accuracy (%)	Time (s)	$P_{mppt}$ (W)	Accuracy (%)	Time (s)	$P_{mppt}$ (W)	Accuracy (%)	Time (s)
1	500.28	499.8	99.91	0.35	499.6	99.86	1.26	497.6	99.48	1.71	500.26	99.99	0.45
2	110.69	91.3	82.48	0.21	110.65	99.96	1.73	109.8	99.2	1.72	110.4	99.74	0.77

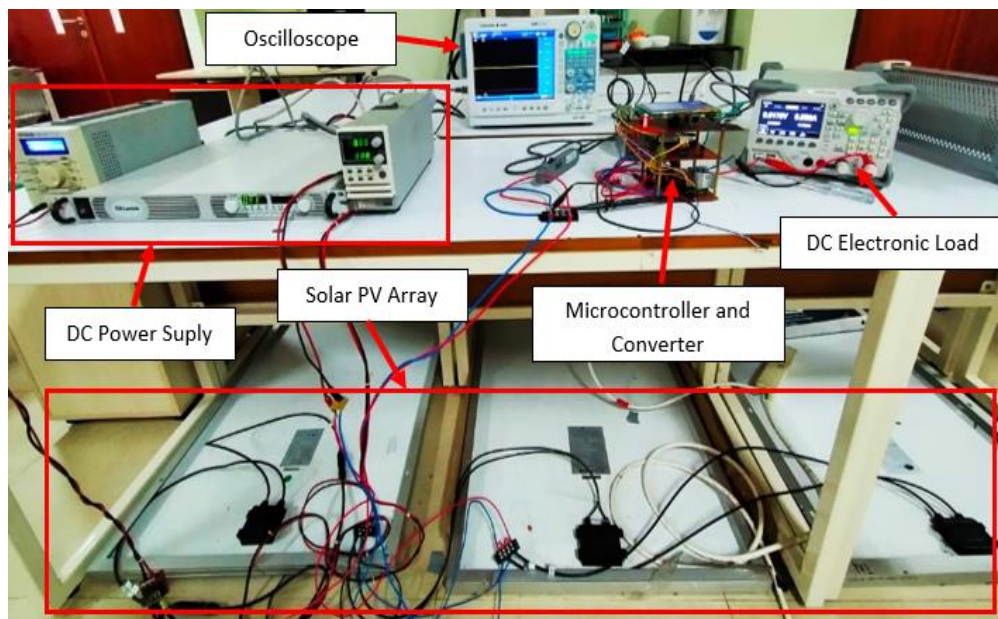
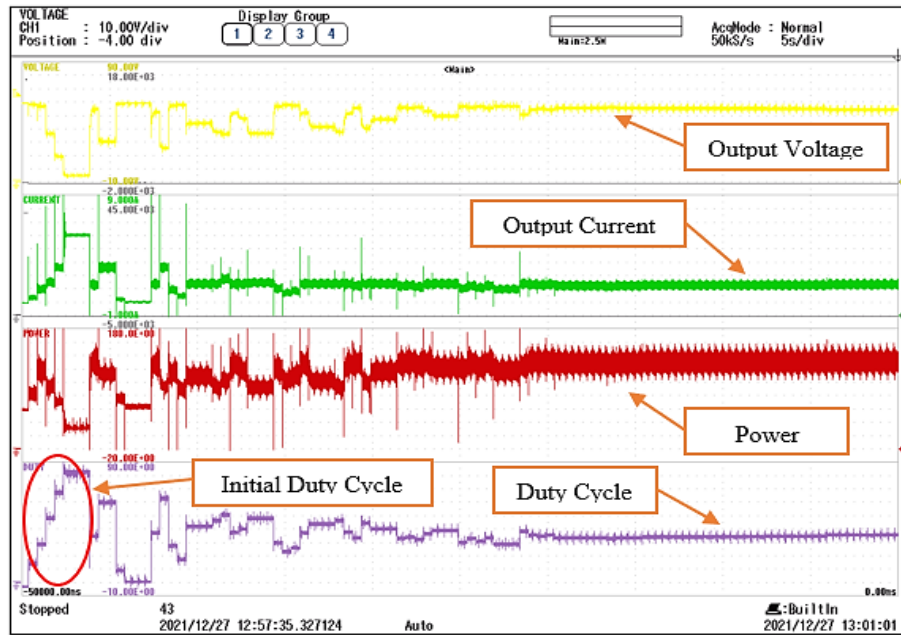
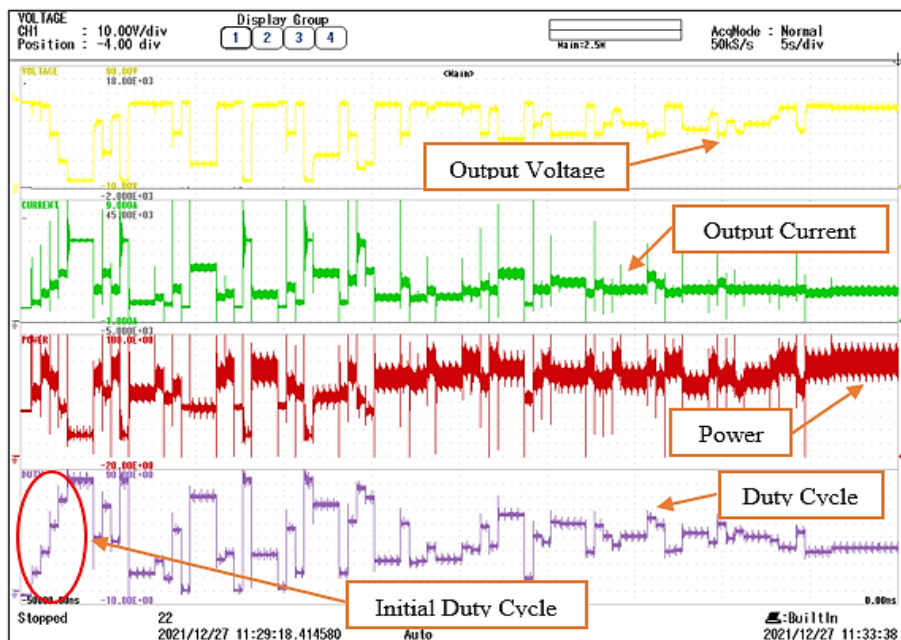


Figure 12. Experimental prototype with unilluminated solar PV of MPPT system



(a)



(b)

Figure 13. PV array output performance under partial shading with non-uniform irradiation  $1000 \text{ W/m}^2$ ,  $600 \text{ W/m}^2$ ,  $400 \text{ W/m}^2$  (a) improved SHO-MPPT and (b) SHO-MPPT

## 6. CONCLUSION

In this study, the proposed SHO-MPPT and improved SHO-MPPT are tested, and other comparison algorithms such as P&O and PSO are used to test the algorithm performance for MPPT under uniform and partial shading. The simulation results show that the best vector  $\vec{h}$  value range for improved SHO-MPPT is (2, 0), there is less fluctuation power, fast to track the MPP and high accuracy. The simulation results show that the P&O-MPPT can track MPP fast, but in MPP condition, there is oscillation, where it can increase power losses. Besides that, when partial shading with non-uniform irradiation, the P&O-MPPT failed to get GMPP and trapped in LMPP. The SHO-MPPT can track the MPP with an accuracy value above 99% and increase the efficiency by reducing oscillations around the MPP. However, before reach MPP, there is

fluctuation power. The improved SHO-MPPT has better performance results than the PSO-MPPT and SHO-MPPT. The improved SHO has an accuracy value above 99%, can reach MPP faster and reduce the power fluctuations better than SHO-MPPT and PSO-MPPT. The experimental results show that the improved SHO-MPPT can track MPP faster and reduce power fluctuation better than SHO-MPPT.

## REFERENCES

- [1] D. C. Momete, "Analysis of the potential of clean energy deployment in the European Union," *IEEE Access*, vol. 6, pp. 54811–54822, 2018, doi: 10.1109/ACCESS.2018.2872786.
- [2] S. Abolhosseini, A. Heshmati, and J. Altmann, "A review of renewable energy supply and energy efficiency technologies," *SSRN Electronic Journal*, 2014, doi: 10.2139/ssrn.2432429.
- [3] M. Wasfi, "Solar energy and photovoltaic systems," *Journal of Selected Areas in Renewable and Sustainable Energy (JRSE)*, pp. 1–8, 2011.
- [4] H. Deboucha, S. Mekhilef, S. Belaid, and A. Guichi, "Modified deterministic jaya (DM-jaya)-based MPPT algorithm under partially shaded conditions for PV system," *IET Power Electronics*, vol. 13, no. 19, pp. 4625–4632, Dec. 2020, doi: 10.1049/iet-pel.2020.0736.
- [5] M. Lasheen, A. K. Abdel Rahman, M. Abdel-Salam, and S. Ookawara, "Adaptive reference voltage-based MPPT technique for PV applications," *IET Renewable Power Generation*, vol. 11, no. 5, pp. 715–722, Apr. 2017, doi: 10.1049/iet-rpg.2016.0749.
- [6] S. Veerapen, H. Wen, and Y. Du, "Design of a novel MPPT algorithm based on the two stage searching method for PV systems under partial shading," in *2017 IEEE 3rd International Future Energy Electronics Conference and ECCE Asia, IFEEC - ECCE Asia 2017*, Jun. 2017, pp. 1494–1498., doi: 10.1109/IFEEC.2017.7992266.
- [7] M. Abdel-Salam, M. T. El-Mohandes, and M. El-Ghazaly, "An efficient tracking of MPP in PV systems using a newly-formulated P&O-MPPT method under varying irradiation levels," *Journal of Electrical Engineering & Technology*, vol. 15, no. 1, pp. 501–513, Jan. 2020, doi: 10.1007/s42835-019-00283-x.
- [8] R. Alik and A. Jusoh, "An enhanced P&O checking algorithm MPPT for high tracking efficiency of partially shaded PV module," *Solar Energy*, vol. 163, pp. 570–580, Mar. 2018, doi: 10.1016/j.solener.2017.12.050.
- [9] C. Manickam, G. P. Raman, G. R. Raman, S. I. Ganesan, and N. Chilakapati, "Fireworks enriched P&O algorithm for GMPPT and detection of partial shading in PV systems," *IEEE Transactions on Power Electronics*, vol. 32, no. 6, pp. 4432–4443, Jun. 2017, doi: 10.1109/TPEL.2016.2604279.
- [10] S. Motahhir, A. El Ghzizal, S. Sebti, and A. Derouich, "Modeling of photovoltaic system with modified incremental conductance algorithm for fast changes of irradiance," *International Journal of Photoenergy*, vol. 2018, pp. 1–13, 2018, doi: 10.1155/2018/3286479.
- [11] P. Shah and B. Singh, "Robust EnKF with improved RCGA-based control for solar energy conversion systems," *IEEE Transactions on Industrial Electronics*, vol. 66, no. 10, pp. 7728–7740, Oct. 2019, doi: 10.1109/TIE.2018.2885727.
- [12] K. S. Tey, S. Mekhilef, M. Seyedmahmoudian, B. Horan, A. T. Oo, and A. Stojcevski, "Improved differential evolution-based MPPT algorithm using SEPIC for PV systems under partial shading conditions and load variation," *IEEE Transactions on Industrial Informatics*, vol. 14, no. 10, pp. 4322–4333, Oct. 2018, doi: 10.1109/TII.2018.2793210.
- [13] S. Mirjalili, S. M. Mirjalili, and A. Lewis, "Grey wolf optimizer," *Advances in Engineering Software*, vol. 69, pp. 46–61, Mar. 2014, doi: 10.1016/j.advengsoft.2013.12.007.
- [14] Y. Wan, M. Mao, L. Zhou, Q. Zhang, X. Xi, and C. Zheng, "A novel nature-inspired maximum power point tracking (MPPT) controller based on SSA-GWO algorithm for partially shaded photovoltaic systems," *Electronics*, vol. 8, no. 6, Jun. 2019, doi: 10.3390/electronics8060680.
- [15] S. Titri, C. Larbes, K. Y. Toumi, and K. Benatchba, "A new MPPT controller based on the Ant colony optimization algorithm for Photovoltaic systems under partial shading conditions," *Applied Soft Computing*, vol. 58, pp. 465–479, Sep. 2017, doi: 10.1016/j.asoc.2017.05.017.
- [16] S. Padmanaban, N. Priyadarshi, M. Sagar Bhaskar, J. B. Holm-Nielsen, V. K. Ramachandaramurthy, and E. Hossain, "A hybrid ANFIS-ABC based MPPT controller for PV system with anti-islanding grid protection: experimental realization," *IEEE Access*, vol. 7, pp. 103377–103389, 2019, doi: 10.1109/ACCESS.2019.2931547.
- [17] H. Li, D. Yang, W. Su, J. Lu, and X. Yu, "An overall distribution particle swarm optimization MPPT algorithm for photovoltaic system under partial shading," *IEEE Transactions on Industrial Electronics*, vol. 66, no. 1, pp. 265–275, Jan. 2019, doi: 10.1109/TIE.2018.2829668.
- [18] A. Fathy, H. Rezk, and D. Yousri, "A robust global MPPT to mitigate partial shading of triple-junction solar cell-based system using manta ray foraging optimization algorithm," *Solar Energy*, vol. 207, pp. 305–316, Sep. 2020, doi: 10.1016/j.solener.2020.06.108.
- [19] K. Kaced, C. Larbes, N. Ramzan, M. Bounabi, and Z. elabidine Dahmane, "Bat algorithm based maximum power point tracking for photovoltaic system under partial shading conditions," *Solar Energy*, vol. 158, pp. 490–503, Dec. 2017, doi: 10.1016/j.solener.2017.09.063.
- [20] G. Dhiman and V. Kumar, "Spotted hyena optimizer: A novel bio-inspired based metaheuristic technique for engineering applications," *Advances in Engineering Software*, vol. 114, pp. 48–70, Dec. 2017, doi: 10.1016/j.advengsoft.2017.05.014.
- [21] N. Pandiarajan and R. Muthu, "Mathematical modeling of photovoltaic module with Simulink," in *1st International Conference on Electrical Energy Systems*, Jan. 2011, pp. 258–263., doi: 10.1109/ICEES.2011.5725339.
- [22] C. R. S. Reinoso, D. H. Milone, and R. H. Buitrago, "Simulation of photovoltaic centrals with dynamic shading," *Applied Energy*, vol. 103, pp. 278–289, Mar. 2013, doi: 10.1016/j.apenergy.2012.09.040.
- [23] K. Ishaque, Z. Salam, A. Shamsudin, and M. Amjad, "A direct control based maximum power point tracking method for photovoltaic system under partial shading conditions using particle swarm optimization algorithm," *Applied Energy*, vol. 99, pp. 414–422, Nov. 2012, doi: 10.1016/j.apenergy.2012.05.026.
- [24] M. C. Di Piazza and G. Vitale, "Photovoltaic field emulation including dynamic and partial shadow conditions," *Applied Energy*, vol. 87, no. 3, pp. 814–823, Mar. 2010, doi: 10.1016/j.apenergy.2009.09.036.
- [25] D. Hart, *Power electronics*. McGraw-Hill Education, 2011.

**BIOGRAPHIES OF AUTHORS**

**Muhammad Farizky Alvianandy**    received the B.Sc. degree in electrical engineering from the Department of Electrical Engineering, Politeknik Elektronika Negeri Surabaya, Indonesian in 2020. Currently, he is pursuing the M.Eng. degree at the same university. His research interest in photovoltaic, battery management system, state of charge, state of health, renewable energy, artificial intelligent, and metaheuristic optimization. He can be contacted at email: pondokmulia@pasca.student.pens.ac.id, fariezky26@gmail.com. pondokmulia@gmail.com.



**Novie Ayub Windarko**    finished his bachelor and master degree from Department of Electrical Engineering, Institut Teknologi Sepuluh Nopember Surabaya, Indonesia. He received his Ph.D from School of Electrical Engineering, Chungbuk National University, South Korea. He was a JICA junior visiting researcher in Hirofumi Akagi Lab., Tokyo Institute of Technology in 2002. He has been joining to PENS since 2000. He was the head of Renewable Energy Research Centre of PENS. He received the best paper and the best poster award at IEEE IES 2015. He has served as reviewers for IEEE Trans. on Transportation Electrification, IEEE Trans. on Power Electronics, Journal of Batteries, Journal of Energies and EMITTER International Journal of Engineering Technology. His research interests include power electronics converter, PV power generation, and optimization for renewable energy. He can be contacted at email: ayub@pens.ac.id.



**Bambang Sumantri**    is a lecturer of Politeknik Elektronika Negeri Surabaya (PENS), Indonesia. He received bachelor degree in Electrical Engineering from Institut Teknologi Sepuluh Nopember (ITS), Indonesia, in 2002, M.Sc. (Master of Science) in Control Engineering from Universiti Teknologi Petronas, Malaysia, in 2009, and Doctor of Engineering in Mechanical Engineering, Toyohashi University of Technology, Japan, in 2015. His research interest is in robust control system, embedded controller, and renewable energy. He can be contacted at email: bambang@pens.ac.id.